

BEYOND HEAVY TOP LIMIT IN HIGGS BOSON PRODUCTION AT LHC

Alexey Pak, Mikhail Rogal, and Matthias Steinhauser
Institut für Theoretische Teilchenphysik (TTP), KIT Karlsruhe

QCD corrections to inclusive Higgs boson production at the LHC are evaluated at next-to-next-to leading order. By performing asymptotic expansion of the cross section near the limit of infinitely heavy top quark we obtained a few first top mass-suppressed terms. The corrections to the hadronic cross sections are found to be small compared to the scale uncertainty, thus justifying the use of heavy top quark approximation in many published results.

1 Introduction

The Large Hadron Collider (LHC) at CERN is expected to provide insights on the mechanism of electroweak symmetry breaking, possibly by discovering the elusive Higgs boson. In the Standard Model, the dominant process of the Higgs boson production is the gluon fusion, $gg \rightarrow H$, mediated by a top quark loop. Predictions of Higgs boson production in gluon fusion both at the Tevatron and the LHC^{1,2} include electroweak effects and results beyond the fixed-order perturbation theory, but QCD corrections have the greatest numerical effect. Since 1977, when the leading order (LO) calculation appeared³, also next-to-leading order (NLO)^{4,5,6}, and more recently next-to-next-to-leading order (NNLO)^{7,8,9,10} QCD corrections have been evaluated.

While the NLO results are exact in the top quark and Higgs boson masses, the NNLO results rely on the effective theory built in the limit of the large top quark mass (for a review see e.g. Ref.¹¹). At NLO, this approximation results in $< 2\%$ deviations from the exact result for $M_H < 2M_t$ ^{12,13}. NNLO effects of the finite top quark mass have been first indirectly addressed in Ref.¹⁴, where the asymptotics in the opposite limit of large center-of-mass energy \sqrt{s} were considered. Recently, two independent groups^{15,16,17} performed an expansion of the inclusive Higgs production cross-section in $\rho = M_H^2/M_t^2$. In this contribution we summarize those results and provide some details of our calculation¹⁶.

2 Calculation of partonic cross-sections

The QCD corrections to the cross-sections of partons are:

$$\hat{\sigma}_{ij \rightarrow H+X} = \hat{A}_{\text{LO}} \left(\Delta_{ij}^{(0)} + \frac{\alpha_s}{\pi} \Delta_{ij}^{(1)} + \left(\frac{\alpha_s}{\pi} \right)^2 \Delta_{ij}^{(2)} + \dots \right), \quad \hat{A}_{\text{LO}} = \frac{G_F \alpha_s^2}{288\sqrt{2}\pi} f_0(\rho, 0). \quad (1)$$

Here ij denote one of the possible initial states: gg , $q\bar{q}$, $q\bar{q}$, qq , or qq' , and q and q' stand for (different) massless quark flavours. At the leading order, the only non-zero contribution is $\Delta_{gg}^{(0)} = \delta(1-x)$, and the function $f_0(\rho, 0)$ ¹⁸ describes the mass dependence. We focus on the

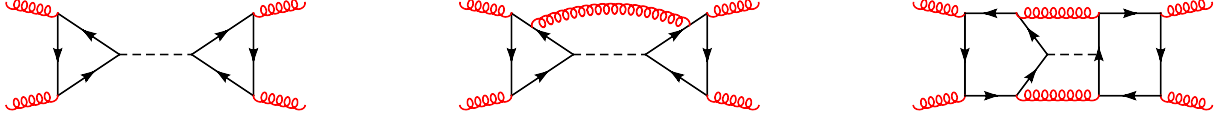


Figure 1: Sample forward scattering diagrams whose cuts correspond to the LO, NLO and NNLO corrections to $gg \rightarrow H$. Dashed, curly and solid lines represent Higgs bosons, gluons and top quarks, respectively.

x - and ρ -dependence of $\Delta_{ij}^{(1)}$ and $\Delta_{ij}^{(2)}$. As is common in the literature, by “infinite top quark mass approximation” we assume that $\Delta_{ij}^{(k)}$ are evaluated for $M_t \rightarrow \infty$, but \hat{A}_{LO} is exact in M_t .

To account for the real and virtual corrections we employ the optical theorem and compute imaginary parts of the four-point forward-scattering amplitudes such as in Fig. 1. After the asymptotic expansion in the limit $M_t^2 \gg \hat{s}, M_H^2$ the loop integrals factorize. The most non-trivial cases are two-loop four-point functions dependent on both \hat{s} and M_H . Reducing them with IBP’s¹⁹ we obtain around 30 master integrals. The latter are available¹⁰, however, we re-computed them with the combination of soft expansion and differential equation methods. Finally, we add renormalization terms and obtain a few first terms in the expansion of $\Delta_{ij}^{(k)}$ in powers of ρ , where coefficients are functions of x .

3 NLO and NNLO results

In Fig. 2 we compare the x -dependence of the exact NLO results^{4,5,6} (evaluated for $M_H = 130$ GeV and $M_t = 173.1$ GeV) to the $\mathcal{O}(\rho^n)$ approximations for successive n . The leading term in ρ is smooth and demonstrates a reasonably good agreement with the exact curve for $x \rightarrow 1$. However, the higher order terms in ρ introduce divergences at $x \rightarrow 0$ which are the most obvious for the $q\bar{q}$ channel. This signifies the breakdown of the assumption that $M_t^2 \gg \hat{s}$ for large \hat{s} . Note, however, the decent convergence above the threshold for the top quark pair production (in Fig. 2, $x_{\text{th}} \approx 0.14$). To recover the proper $x \rightarrow 0$ behaviour, we utilize $\hat{s} \rightarrow \infty$ asymptotics^{14,17}. Interpolation between the $\mathcal{O}(\rho^n)$ result and the value at $x \rightarrow 0$ (dots in Fig. 2) agrees well with the exact curve for the gg channel. For the quark channels, the introduced error in hadronic contributions does not exceed 50%, which, if also true at NNLO, translates to a shift less than the total scale uncertainty of the full NNLO cross-section.

The NNLO diagrams require considerably more effort. Using the known virtual corrections^{17,18} we were able to evaluate three terms in the expansion of $\Delta_{gg}^{(2)}$ and four terms in the other channels. Our analytic results are in full agreement with the $M_t \rightarrow \infty$ results¹⁰ and the mass corrections expanded in $(1-x)$ (soft expansion)^{15,17}. In Fig. 3 we present x -dependence of the functions $\Delta_{gg}^{(2)}$, $\Delta_{qg}^{(2)}$, and $\Delta_{q\bar{q}}^{(2)}$, with interpolations constructed similarly to the NLO case.

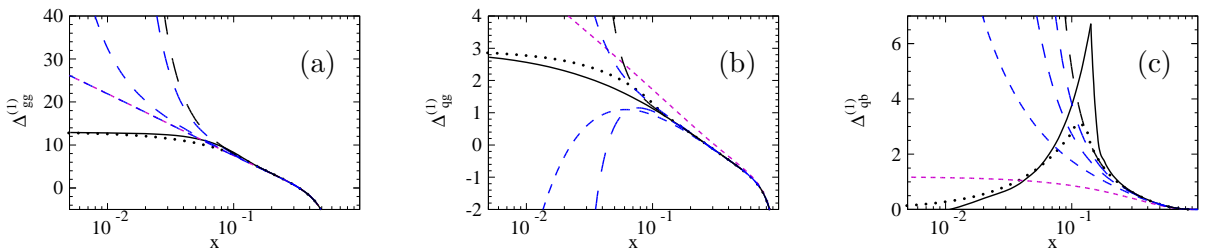


Figure 2: NLO partonic cross sections for the (a) gg , (b) qg and (c) $q\bar{q}$ channel as functions of x for $M_H = 130$ GeV. The expansion in $\rho \rightarrow 0$ (dashed lines) is compared with the exact result (solid lines). Lines with longer dashes include higher order terms in ρ . The interpolation (see text) is shown as a dotted line.

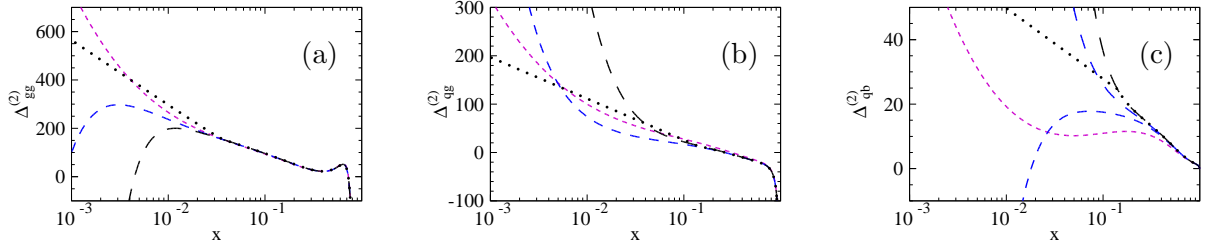


Figure 3: Partonic NNLO cross sections for the (a) gg , (b) qq , (c) $q\bar{q}$ channels for $M_H = 130$ GeV. Lines with longer dashes include higher order terms in ρ . Dotted lines corresponds to interpolation.

4 Hadronic results

The hadronic cross sections are given by the convolution of $\hat{\sigma}_{ij \rightarrow H+X}$ with the corresponding parton distribution functions (PDFs). We decompose it into LO, NLO, and NNLO contributions: $\sigma_{pp' \rightarrow H+X}(s) = \sigma^{\text{LO}} + \delta\sigma^{\text{NLO}} + \delta\sigma^{\text{NNLO}}$. In Fig. 4 we show the M_H -dependence of $\delta_{qg}^{(2)}$, $\delta_{q\bar{q}}^{(2)}$, and $\delta_{qq}^{(2)}$ normalized to the infinite top quark mass result, labeled with subscript ∞ . In all cases the power-suppressed terms lead to an increase of the cross section between 4% and 10% for the quark-gluon and up to 25% for the quark-anti-quark channel in our range of Higgs boson masses. For the qq and qq' channels we observe rapid convergence beyond $1/M_t^2$.

NNLO corrections to the gg channel are shown in Fig. 5(a). Finally, in Fig. 5(b) we present the gluon-induced cross-section including exact LO and NLO contributions. Minor differences with the left panel of Fig. 7 in Ref. ¹⁵ can be attributed to the different matching procedure. As one can see, the effects of matching near $x = 0$ and M_t -suppressed corrections nearly cancel and the final deviation from the heavy top mass result is below 1% (when exact LO mass dependence is factored out).

5 Conclusion

We present the NNLO production cross section of the Standard Model Higgs boson including the finite top quark mass effects. To improve $x \rightarrow 0$ behaviour for the gluon-gluon channel we match our results to the $\hat{s} \rightarrow \infty$ limit. The numerical impact of the top quark mass suppressed terms is below 1% and thus about a factor of ten smaller than the scale variation uncertainty. Our calculation justifies the use of the heavy top quark mass approximation in NNLO cross section calculations. In addition, we independently confirm the analytic results in the heavy top limit ¹⁰ and the soft expansion of M_t -suppressed terms ¹⁵.

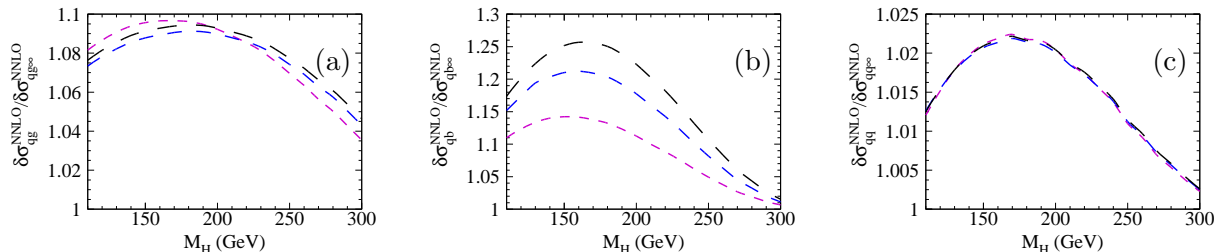


Figure 4: NNLO contributions to hadronic cross section with higher orders in $1/M_t$ (from short to long dashes) normalized to the heavy top quark mass result, (a) gg , (b) $q\bar{q}$, (c) qq . Channels qq' and qq are almost identical.

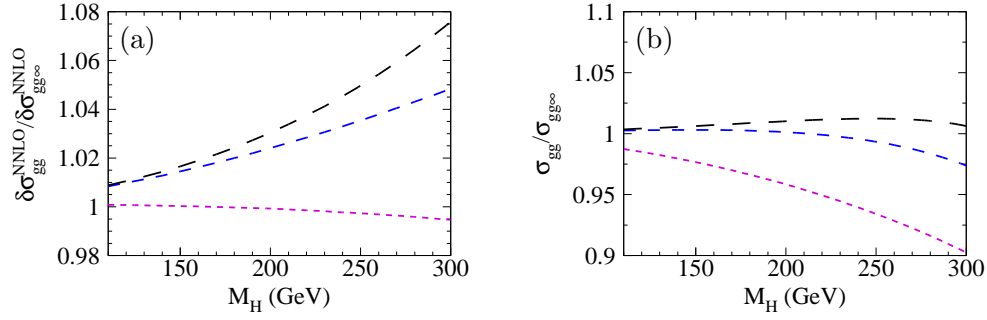


Figure 5: (a) Ratio of the NNLO hadronic cross section (gg contribution) including successive higher orders in $1/M_t$ normalized to the infinite top quark mass result. (b) Prediction for the gluon-induced inclusive Higgs production cross section up to NNLO normalized to the heavy top limit.

Acknowledgements. This work was supported by the DFG through the SFB/TR 9 “Computational Particle Physics”. M.R. was supported by the Helmholtz Alliance “Physics at the Terascale”.

References

1. D. de Florian and M. Grazzini, Phys. Lett. B **674** (2009) 291, arXiv:0901.2427 [hep-ph].
2. C. Anastasiou, R. Boughezal, and F. Petriello, JHEP **04** (2009) 003, arXiv:0811.3458 [hep-ph].
3. F. Wilczek, Phys. Rev. Lett. **39** (1977) 1304; J. R. Ellis, M. K. Gaillard, D. V. Nanopoulos and C. T. Sachrajda, Phys. Lett. B **83** (1979) 339; H. M. Georgi, S. L. Glashow, M. E. Machacek and D. V. Nanopoulos, Phys. Rev. Lett. **40** (1978) 692; T. G. Rizzo, Phys. Rev. D **22** (1980) 178 [Addendum-ibid. D **22** (1980) 1824].
4. S. Dawson, Nucl. Phys. B **359** (1991) 283;
5. M. Spira, A. Djouadi, D. Graudenz and P. M. Zerwas, Nucl. Phys. B **453** (1995) 17; arXiv:hep-ph/9504378;
6. A. Djouadi, M. Spira and P. M. Zerwas, Phys. Lett. B **264** (1991) 440.
7. R. V. Harlander, Phys. Lett. B **492** (2000) 74, arXiv:hep-ph/0007289;
8. R. V. Harlander and W. B. Kilgore, Phys. Rev. Lett. **88** (2002) 201801, arXiv:hep-ph/0201206;
9. V. Ravindran, J. Smith and W. L. van Neerven, Nucl. Phys. B **665** (2003) 325, arXiv:hep-ph/0302135.
10. C. Anastasiou and K. Melnikov, Nucl. Phys. B **646** (2002) 220, arXiv:hep-ph/0207004.
11. M. Steinhauser, Phys. Rept. **364** (2002) 247, arXiv:hep-ph/0201075.
12. R. Harlander, Eur. Phys. J. C **33** (2004) S454 arXiv:hep-ph/0311005.
13. M. Kramer, E. Laenen, M. Michael, Nucl. Phys. B **B511** (1998) 523-549, arXiv:hep-ph/9611272;
14. S. Marzani, R. D. Ball, V. Del Duca, S. Forte and A. Vicini, Nucl. Phys. B **800** (2008) 127 arXiv:0801.2544 [hep-ph].
15. R. V. Harlander and K. J. Ozeren, arXiv:0909.3420 [hep-ph].
16. A. Pak, M. Rogal and M. Steinhauser, arXiv:0911.4662 [hep-ph].
17. R. V. Harlander and K. J. Ozeren, Phys. Lett. B **679** (2009) 467 arXiv:0907.2997 [hep-ph].
18. A. Pak, M. Rogal and M. Steinhauser, Phys. Lett. B **679** (2009) 473 arXiv:0907.2998 [hep-ph].
19. S. Laporta, Int. J. Mod. Phys. A **15** (2000) 5087, arXiv:hep-ph/0102033.
20. R. V. Harlander, H. Mantler, S. Marzani and K. J. Ozeren, arXiv:0912.2104 [hep-ph].